

THE “TRUE” BENDING STRESS in SPUR GEARS

Edoardo Conrado and Piermaria Davoli

Management Summary

It is well known from the literature that the true bending stresses at the tooth root of spur gears are quite different from the nominal values that are utilized for the calculation of load capacity, either by standards or usual design rules.

No problems arise in using a load capacity rating when the simplified values are compared with the results of bending fatigue tests whose limits are calculated with the same schematic method.

But the “true” stress at the tooth root has different trends and values, and the designer must be aware of this difference, especially for light gears with narrow ribs and rims.

In this paper, an accurate FEM analysis has been done of the “true” stress at tooth root of spur gears in the function of the gear geometry. The obtained results confirm the importance of these differences.

Introduction

In today’s gear industry, designers typically utilize rating methods of gear load capacity based on standards or the customary design rules. In these methods, nominal quantities are calculated in order to characterize the stress field in the gear. These nominal quantities are compared with limit values derived from tests using gears as specimens.

In the case of tooth bending strength, a cantilever-beam model is generally used to compute the bending stress. With this approach, Lewis in 1892 first calculated the tooth root stress of spur gear teeth (W. Lewis, “Investigation of the Strength of Gear Teeth,” *Proceedings of Engineers Club*, Philadelphia). This model is still the basis for standard calculation methods successfully used in gear design. However, the local stress state—the “true” stress—in the tooth root fillet may be different from the nominal values obtained by this method.

In truth, the calculation of the maximum tensile stress at the tooth root is a three-dimensional problem: The plane strain or plane stress model can be used without approximations only in the case of infinite, or infinitesimal, face width. In Reference 1, starting from the analytical solution of Jaramillo (Ref. 2), Wellauer and Seireg introduced a study of the bending stress of gear teeth based on a cantilever-plate model. This method shows clearly that a three-dimensional model must be used to evaluate the variation of the tooth root stress along the face width. Current numerical methods, FEM and BEM, for example, are available for the solution of the elasticity problem for complex domains. Thus it is possible to calculate accurately the local strain and stress state in the tooth root, taking into account the real geometry of both gear

Table 1- Synthesis of the cases analyzed for the full-body and the thin-rimmed gear.

	Full-Body Gears	Thin-Rimmed Gears
Model	Single Gear	Gear Pair
Load	Pinion	Pinion
Body Gear Structure	Full Rim	Rim Supported by a Web
Geometric Parameters	Module $m=4.5$ mm Face width $b = 5, 10, 15, 20, 30, 40, 50, 70, 100$ mm and Plane Strain Condition.	Module $m=4.5$ mm Face width $b=20$ mm Backup ratio $r = 0.5 - 0.65 - 0.75$ Web ratio $w = 0.2 - 0.3 - 0.4$
Gear Data For Pinion		
Normal Module	m_n	
Number of Teeth	z	
Normal Pressure Angle	α_n	
Tip Diameter	d_a	
Root Diameter	d_R	
Profile Shift Coefficient	x	
Span Measurement	W	
Number of Teeth Spanned	k	
Operating Center Distance	a_w	
Tool Geometry		
Tool Normal Tooth Thickness	S_{n0}	
Tool Addendum	h_{a0}	
Tool Addendum	ρ_{a0}	
Tool Protuberance	δ_{a0}	

teeth and body (Refs. 3 and 4).

This work analyzes the stress field at the tooth root using a three-dimensional, parametric, finite element solid model. Commonly used gear geometries having full body and thin-rimmed body connected to the hub by a web are also analyzed.

Full Body Gear

The methods that are commonly used for the calculation of gear-bending strength are based on a cantilever-beam model. The maximum tensile stress in the tooth root is therefore computed in a plane strain condition for an error-free gear pair. The influence of the face width and the variation of the tooth root stress along the gear width is not taken into account.

This study examines the bending stress along the tooth width for a fixed geometry and for different values of face width (Table 1). To begin, the case of an error-free spur gear pair with full body was considered. In the FEM analyses, only half of the pinion was modeled, since loading conditions and geometry are symmetrical to the middle plane of the gear width (Fig. 1). The load, applied at the highest point of single tooth contact (HPSTC), was modeled as a linear force uniformly distributed along the face width and perpendicular to the tooth surface. The hub of the pinion was fixed (Fig. 1). An example of the FE models used in the analyses is shown in Figure 2.

Even with uniform load along the face width, numerical results show that there are areas with different stress levels at the tooth root (Figs. 3 and 4). For values of the ratio b/m between the face width and the module commonly used in practical gear design, the stress level is higher in the middle of the gear width than in the side areas. In the center cross-section, the magnitude of the maximum principal stress is higher than on the sides of the gear, and an intermediate principal stress is present. In addition, the location of the highest value of the maximum principal stress in each cross-section changes along the face width, but the range is small. The location varies from 30° in the middle

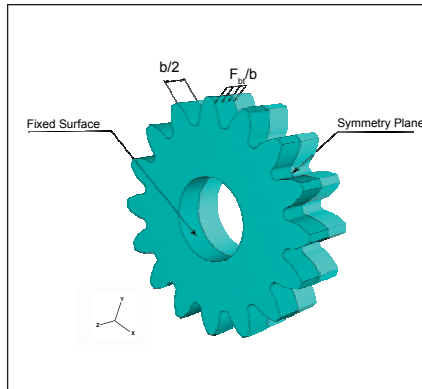


Figure 1—Geometric model and boundary conditions: Full-body gear.

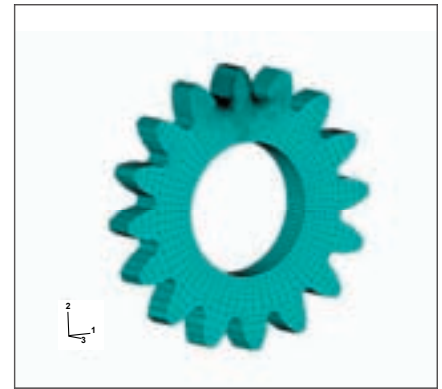


Figure 2—Finite Element Model: Full-body gear.

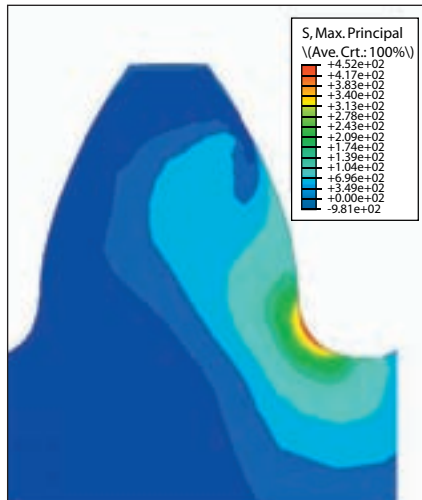


Figure 3—Maximum principal stress contour plot in the middle cross-section: Full-body gear with $b = 20$ mm.

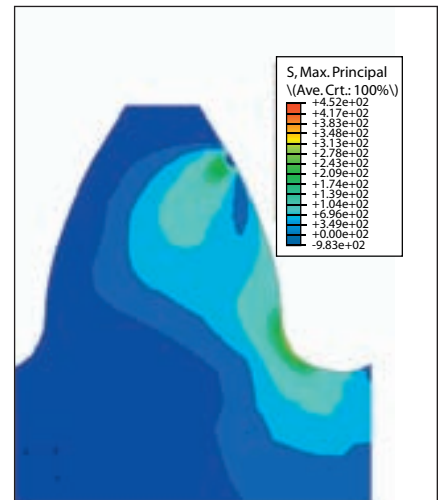


Figure 4—Maximum principal stress contour plot in the side of the gear: Full-body gear with $b = 20$ mm.

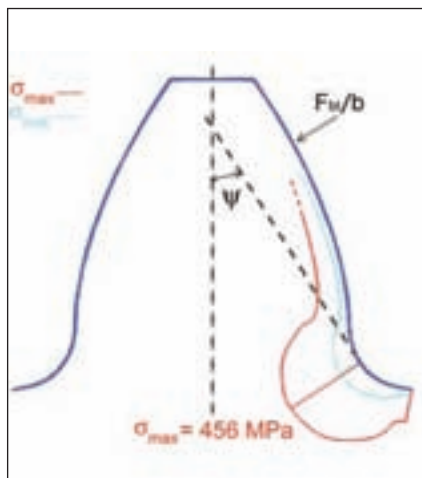


Figure 5—Maximum and intermediate principal stress distribution at the tooth root fillet in the middle cross-section: Full-body gear with $b = 20$ mm.

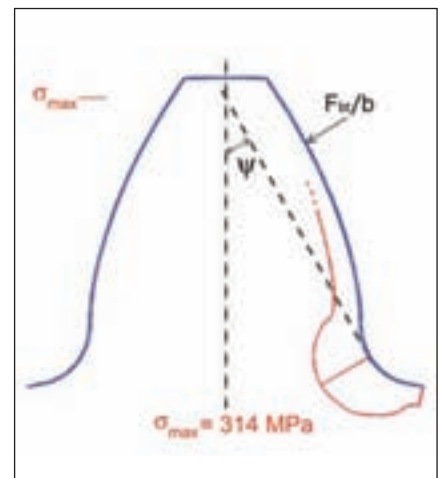


Figure 6—Maximum and intermediate principal stress distribution at the tooth root fillet in the sides of the gear: Full-body gear with $b = 20$ mm.

cross-section to 34° on the sides (Figs. 5 and 6) if the position in the tooth root fillet is described by the angle ψ , the angle between the symmetry line of the tooth and the tangent to the fillet curve.

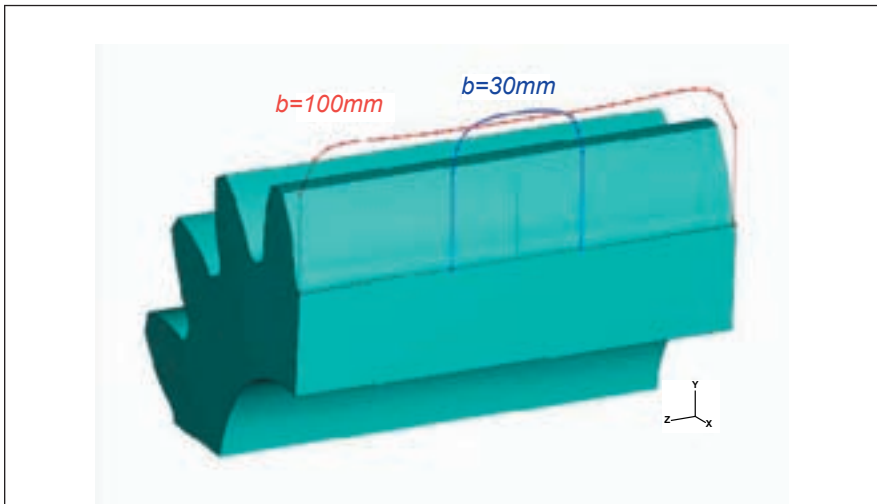


Figure 7—Bending stress distributions along the face width for full-body gears with $b = 30$ mm and $b = 100$ mm.

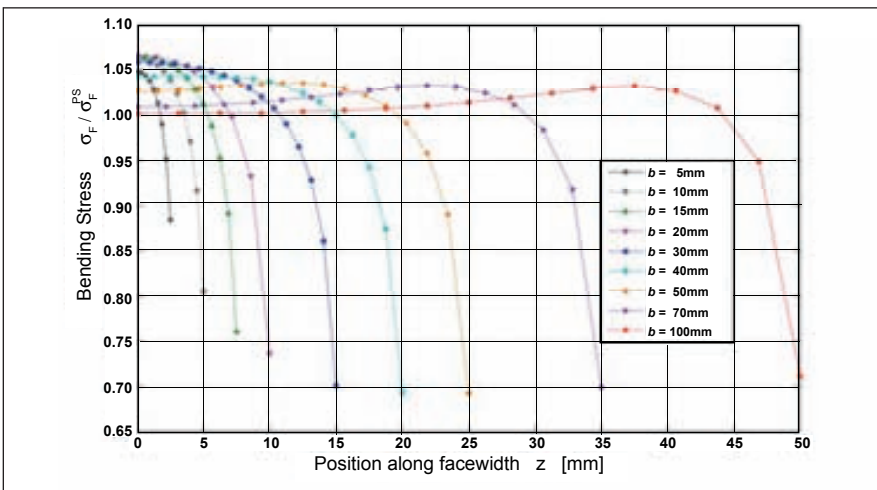


Figure 8—Bending stress distribution along the face width for different b : Full-body gear (σ_F is the bending stress stress and σ_F^{PS} is the bending stress in plane strain condition).

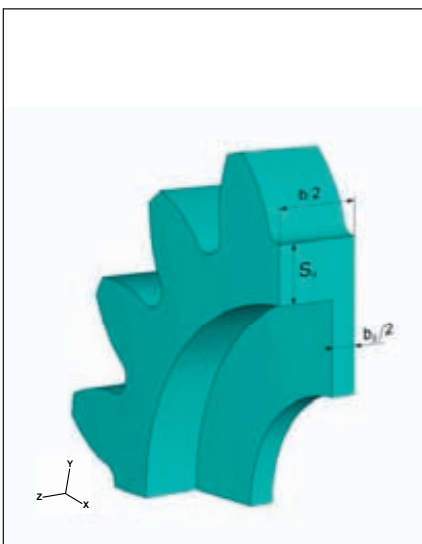


Figure 9—Thin-rimmed gear geometry.

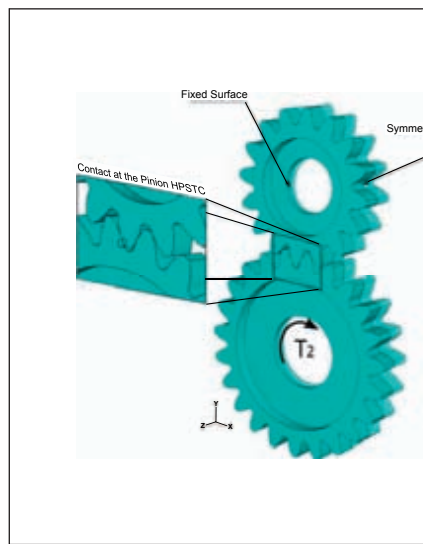


Figure 10—Geometric model and boundary conditions: Thin-rimmed gear.

The highest value of the maximum principal stress in a cross-section—herein named bending stress—may be used to characterize the stress levels along the face width. Figure 7 shows the bending stress as a function of the distance z from the middle plane for gears having different face width. Two types of distribution can be recognized, as shown in Figure 8. For a b/m ratio lower than nine, the maximum of the bending stress is in the middle section and the minimum in the sides of the gear. The maximum is higher than the bending stress calculated in plane strain condition. For a b/m ratio higher than nine, the minimum bending stress is again in the sides of the gear, but the maximum is close to the sides, not in the center. In the middle cross-section, the bending stress approaches the plane strain value for face width close to infinity.

Thin-Rimmed Gears

A common design goal for gears in some power transmissions (e.g., aerospace transmissions) is reduced weight. To meet this goal, thin rims are often utilized. But rims that are too thin may adversely affect the bending stress. Several researchers have employed FEA for the purpose of assessing the influence of the rim thickness on the stress behavior in thin-rimmed gears. Yet most of these 2-D and 3-D analyses do not consider a web structure of the gear body. It is therefore believed that these models cannot give an accurate evaluation of the stress field at the tooth fillet of gears having a thin rim supported by a web.

A model of a spur gear pair is used here to evaluate the influence of both the rim and web thickness. In the geometrical model, the gear bodies are modeled as a thin rim supported by a web (Fig. 9). Nine different case studies are analyzed with all geometry parameters fixed, excepting the back-up ratio and the web thickness ratio (Table 1). The first, here referred to as r , is the ratio between the rim thickness S_r and the tooth height. The second, referred to as w , is the ratio between the web thickness b_s and the face width b .

As opposed to the full-body gear case, the gear pair is modeled and the dry contact of the mating tooth surfaces is simulated by a numerical algorithm. The gear pair position is chosen to load the pinion tooth at the HPSTC, as in the full-body gear analyses. To impose kinematic and static boundary conditions, the pinion hub is fixed and the torque applied to the wheel hub (Fig. 10).

The contact pressure distributions obtained from the numerical simulations were similar in all cases analyzed. The contact pressure was not uniformly distributed along the face width. In the middle section, the pressure distribution is close to the Hertzian distribution for the plane strain condition (Fig. 11). In the side sections, the contact pressure distribution is again elliptical, but the maximum value is lower than in the middle section. This reduction occurs due to the free expansion of the material on the sides of gear, contrary to the middle section. The ratio between the maximum contact pressure in the side and in the middle sections can be calculated according to Johnson (Ref. 6) as $p/p_H = (1-\nu^2) = 0.91$ (considering steel gears). This value is close to that obtained from the analysis $p/p_H = 0.88$ (Fig. 11).

Considering the stress field at the tooth root, the results of the FEAs again show that the maximum bending stress is located in the central cross-section, and the minimum in the sides of the gear. But the difference between these two values is larger than in the full-body gear case. Moreover, the shapes of the maximum principal stress contour lines are different in the two positions along the gear width (Figs. 12 and 13). This is due to the differences between the stiffness of the central area—supported by the rim and the web—and the stiffness of the end areas which are supported only by the rim. As a consequence, the locations of the highest value of the maximum principal stress in the tooth fillet are also different in the two cross-sections; the location varies from 43° in the middle to 32° on the sides (Figs. 14 and 15).

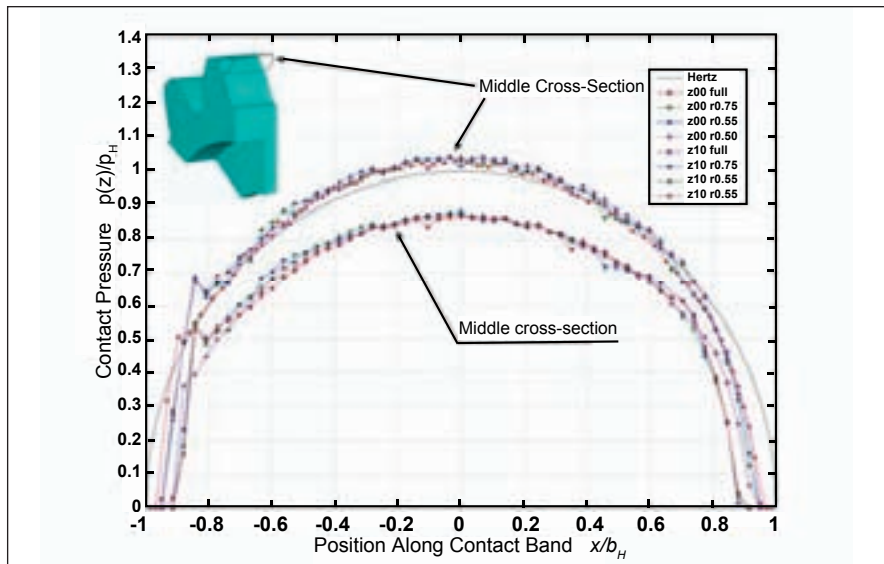


Figure 11—Contact pressure along the involute profile in the middle cross-section (z00) and in the sides of the gear (z10): Thin-rimmed gear with $b=20$ mm, $w=0.3$ and $r=0.5, 0.65$ and 0.75 .

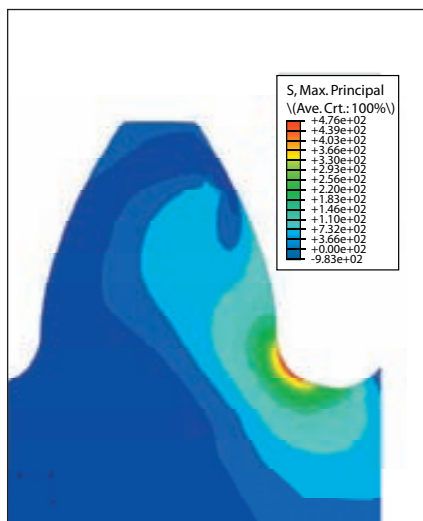


Figure 12—Maximum principal stress contour plot in the middle cross-section: Thin-rimmed gear with $b = 20$ mm, $r = 0.65$ and $w = 0.3$.

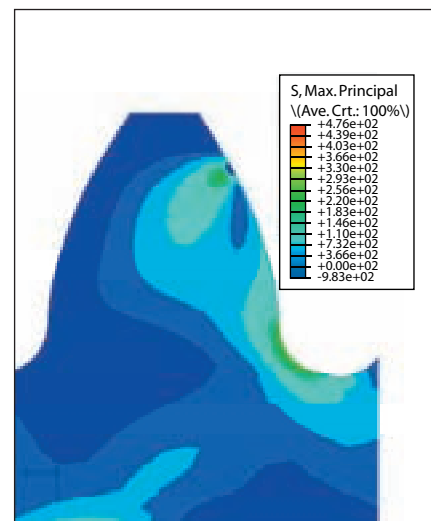


Figure 13—Maximum principal stress contour plot in the middle cross-section: Thin-rimmed gear with $b = 20$ mm, $r = 0.65$ and $w = 0.3$.

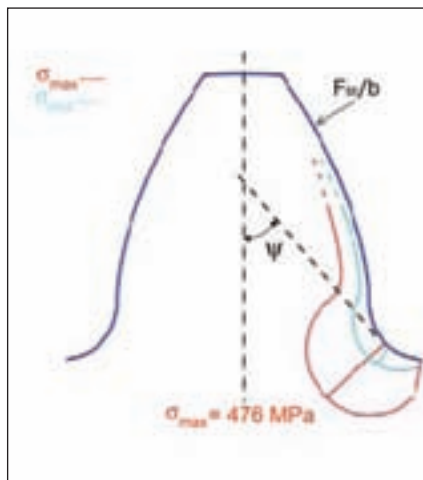


Figure 14—Maximum principal stress at the tooth root fillet in the middle cross-section: Thin-rimmed gear with $b = 20$ mm, $r = 0.65$ and $w = 0.3$.

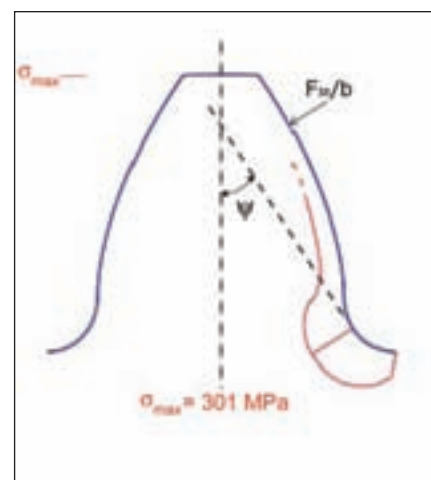


Figure 15—Maximum principal stress at the tooth root fillet in the middle cross-section: Thin-rimmed gear with $b = 20$ mm, $r = 0.65$ and $w = 0.3$.

AGMA and ISO Thin-Rim Coefficients

Both the ISO and AGMA standards (Refs. 7 and 8) introduce stress-modifying factors for the bending stress calculation where the rim thickness is not sufficient to provide full support of the tooth root. The AGMA and ISO rim thickness factors KB and YB have the same meaning and same values as a function of the back-up ratio.

According to the ISO standard, the rim thickness factor should be defined as the ratio of the nominal tooth root stress for a thin-rimmed gear and for a full-body gear with the same geometry but without the back-up ratio. The magnitude of the rim thickness factor can be derived from diagrams (Fig. 17) or calculated according to the ISO standard with this formula for an assigned backup ratio: $YB = 1.6 \ln(2.242 \cdot h_t / S_R)$ per $0.5 < S_R/h_t < 1.2$

The values of the YB factor calculated for $r = 0.5, 0.65$ and 0.75 are listed in Table 2, while the ratio between bending stress for the full-body gear and the thin-rimmed gears investigated in this study are reported in Table 3. The differences between the values for a given r are large, but the effect of web is not taken into account in the YB factor. The values obtained have instead a good correlation with the results of numerical and experimental investigations described in Reference 5, where the effect of both the thin rim and the web thickness are considered.

Conclusions

This paper presents the results of an investigation on the variation of the tooth root stress field along the face width for full-body and thin-rimmed gears. The results of parametric, 3-D finite element analyses are used to characterize the influence of some significant geometric parameters on the bending stress distribution.

For full-body gears, the influence of the face width was investigated, showing areas with different stress levels along the tooth width. The results show that, for face width ratio close to practical gear design, most of the bending stress occurs in the center cross-section

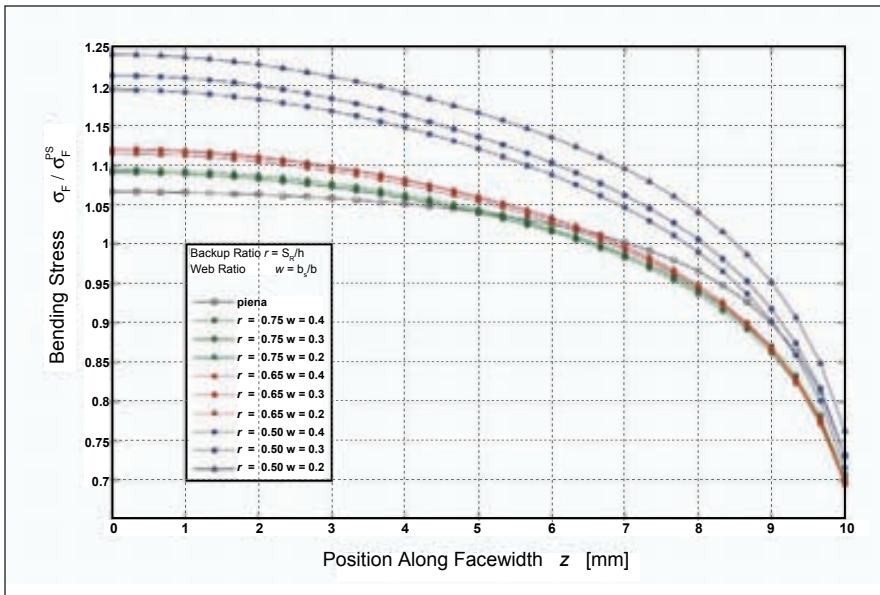


Figure 16—Bending stress distributions along the face width for different r and w : Thin-rimmed gear with $b = 20$ mm (σ_F is the bending stress and σ_F^{PS} is the bending stress in plane strain condition).

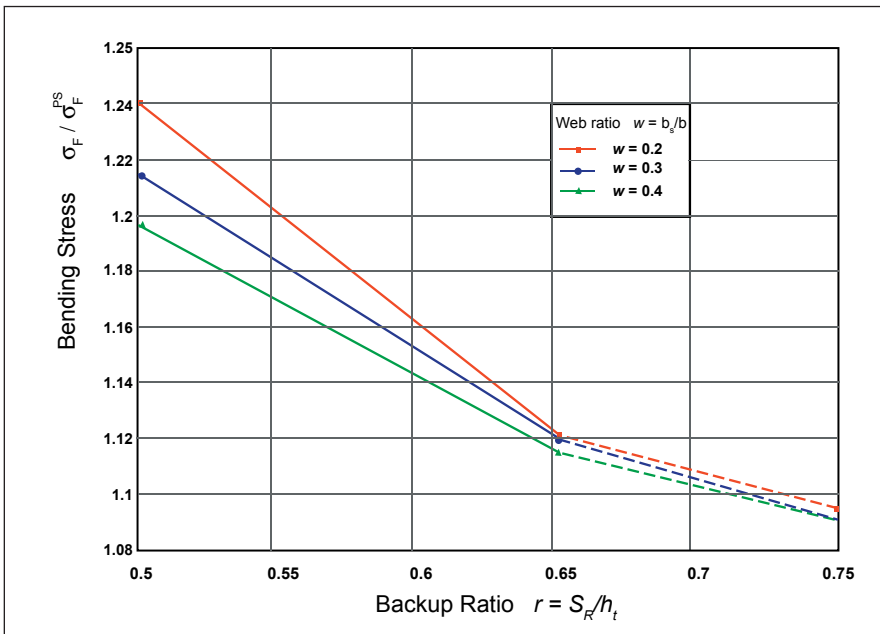


Figure 17—Ratio between the maximum bending stress and the bending stress in plane strain condition as function of the backup ratio for different web thickness ratios.

In Figure 16, the bending stress is plotted as a function of the distance of the section from the middle plane for the nine case studies and for a full-body gear case. For back-up ratio equal to 0.75, the thin rim has a small influence on the bending stress, and the stress distribution is unaffected by web thickness ratio. If the back-up ratio decreases, the magnitude of the bending stress in the middle plane increases and the effect of the web thickness becomes clear—the increment of the bending stress becomes larger when the web thickness decreases (Fig. 16).

and the magnitude is higher than in the plane strain condition. The location in the tooth root fillet of the highest value of the maximum principal stress changes along the face width, but the values of the angle ψ are close to 30° .

For thin-rimmed gears, the influence of both rim and web thickness was investigated. The results show that for backup ratio values larger than 0.75, there is a very small influence on the tooth root stress, while the maximum fillet stress increases sharply as the backup ratio value is smaller than 0.75. Moreover, the more the web thickness is increased, the more the stress concentration factor decreases. 

References

- Wellauer, E. J. and A. Seireg, "Bending Strength of Gear Teeth by Cantilever-Plate Theory," *Journal of Engineering for Industry*, 1960.
- Jaramillo, T. J., "Deflection and Moments Due to a Concentrated Load on a Cantilever Plate of Infinite Length," *Journal of Applied Mechanics*, vol. 17, Trans. ASME, vol. 72, 1950, pp. 67-72.
- Shijun Ma and Chien-ann Hou, "The Crack Initiation of Spur Gear Tooth: Experiments and Analysis," International Gearing Conference, 1988.
- Tsai S. J., and S. H. Wu, "Experimental and Numerical Root Stress Analysis of Conical Gears," International Conference on Gears, München, VDI Berichte, 2005.
- Blazakis, C. A. and D. R. Houser, "Finite Element and Experimental Analysis of the Effects of Thin-Rimmed Gear Geometry on Spur Gear Fillet Stresses," International Gearing Conference, Newcastle-Upon-Tyne, 1994.
- Johnson, K. L., *Contact Mechanics*, Cambridge University Press, 1985.
- ISO 6336:2006 (E), "Calculation of Load Capacity of Spur and Helical Gears," ISO International Standard, 2006.
- ANSI/AGMA 2001-C95, "Fundamental Rating Factors and Calculation Methods for Involute Spur

Table 2— Y_B values as a function of the backup ratios analyzed in this study.			
S_R/h_t	$r = 0.5$	$r = 0.65$	$r = 0.75$
Y_B	2.40	1.98	1.75

Table 3—Ratio between the bending stresses calculated for the thin-rimmed gear and in plane strain condition as a function of the backup ratio $r = S_R/h_t$ and the web thickness ratio $w = b_s/b$.			
σ_F/σ_F^{PS}	$r = 0.5$	$r = 0.65$	$r = 0.75$
$w = 0.2$	1.24	1.12	1.09
$w = 0.3$	1.21	1.21	1.09
$w = 0.4$	1.20	1.11	1.09

and Helical Gear Teeth."

9. Hibbit, Karlsson & Sorensen, Inc. *ABAQUS User's Manual*, version 6.5.

Appendix

The numerical simulations were performed using *ABAQUS* version 6.5-1 in the pre/post processing (*ABAQUS/CAE*) and in the numerical analysis (*ABAQUS/Standard*).

The material was considered homogeneous and isotropic with a linear elastic behavior. Small displacement hypothesis was assumed for the analyses. In the full body gear analyses, hexahedral quadratic elements (3D) and bilinear quadrilateral (2D) elements fully integrated (*ABAQUS* codes C3D20 and CPE8 according to Ref. 9) were used for the domain discretization in the three- and two-dimensional models. In the thin-rimmed gears analyses, hexahedral linear elements (*ABAQUS* code C3D8I according to Ref. 9) were used for the mesh. These types of elements are suggested for the convergence of the contact algorithm and the elements are enhanced by incompatible modes to improve their bending behavior. The number of elements used was varied depending upon the particular gear width being considered.

In the analyses where the gear pair was simulated, the contact between the tooth surfaces was considered as a dry frictionless contact assuming small sliding between the surfaces. The contact constraint was simulated by the LaGrange Multiplier Method (i.e. using the *ABAQUS* option "Hard contact").

Piermaria Davoli is a full professor of machine design at the Department of Mechanical Engineering, Politecnico di Milano, Italy. His research areas include gear transmissions, surface and bending fatigue of gears, and noise emission.

Edoardo Conrado holds a master of science degree in mechanical engineering and is pursuing his Ph.D. in mechanical engineering at Politecnico di Milano, Italy.